Cite this: DOI: 10.1039/c1sm05793f

www.rsc.org/softmatter

PAPER

High performance additive manufactured scaffolds for bone tissue engineering application†

M. Tarik Arafat,[ae] Christopher X. F. Lam,[b] Andrew K. Ekaputra,[b] Siew Yee Wong,[a] Chaobin He,[ac] Dietmar W. Hutmacher,[d] Xu Li*[a] and Ian Gibson*[e]

Received 1st May 2011, Accepted 25th May 2011
DOI: 10.1039/c1sm05793f

This study demonstrates the feasibility of additive manufactured poly(ε-caprolactone)/silanized tricalcium phosphate (PCL/TCP(Si)) scaffolds coated with carbonated hydroxyapatite (CHA)-gelatin composite for bone tissue engineering. In order to reinforce PCL/TCP scaffolds to match the mechanical properties of cancellous bone, TCP has been modified with 3-glycidoxypropyl trimethoxysilane (GPTMS) and incorporated into PCL to synthesize a PCL/TCP(Si) composite. The successful modification is confirmed by X-ray photoelectron spectroscopy (XPS) and Fourier transform infrared spectroscopy (FTIR) analysis. Additive manufactured PCL/TCP(Si) scaffolds have been fabricated using a screw extrusion system (SES). Compression testing demonstrates that both the compressive modulus and compressive yield strength of the developed PCL/TCP(Si) scaffolds fall within the lower ranges of mechanical properties for cancellous bone, with a compressive modulus and compressive yield strength of 6.0 times and 2.3 times of those of PCL/TCP scaffolds, respectively. To enhance the osteoconductive property of the developed PCL/TCP(Si) scaffolds, a CHA-gelatin composite has been coated onto the scaffolds *via* a biomimetic co-precipitation process, which is verified by using scanning electron microscopy (SEM) and XPS. Confocal laser microscopy and SEM images reveal a most uniform distribution of porcine bone marrow stromal cells (BMSCs) and cell-sheet accumulation on the CHA-gelatin composite coated PCL/TCP(Si) scaffolds. The proliferation rate of BMSCs on the CHA-gelatin composite coated PCL/TCP(Si) scaffolds is 2.0 and 1.4 times higher compared to PCL/TCP(Si) and CHA coated PCL/TCP(Si) scaffolds, respectively, by day 10. Furthermore, the reverse transcription polymerase chain reaction (RT-PCR) and western blot analyses reveal that CHA-gelatin composite coated PCL/TCP(Si) scaffolds stimulate osteogenic differentiation of BMSCs the most compared to the other scaffolds. *In vitro* results of SEM, confocal microscopy and proliferation rate also show that there is no detrimental effect of GPTMS modification on biocompatibility of the scaffolds.

Introduction

Despite the high regenerative capacity of bone, large bone defects due to high energy trauma, bone tumor resections, congenital malfunction and severe non-union fractures require a bone substitute for regeneration, which is about 10% of all orthopaedic operations worldwide.[1] Common clinical bone substitutes include xenograft, allograft and autogenous cancellous bone graft from the ilium, chest or tibial tuberosity. Autogenous cancellous bone graft is the most common bone substitute because of its biological properties and lack of possibility of disease transmission or host rejection.[2] Nevertheless, its use is severely hampered by its short supply, temporary disruption of the donor site bone structure and considerable donor site morbidity associated with the harvest.[2,3] Therefore, the development of a new synthetic bone substitute or scaffold that could be used instead of autogenous cancellous bone graft, has become a key research topic in bone tissue engineering.[4–7]

An ideal scaffold aims to mimic the mechanical and biochemical properties of the native tissue. Therefore, one fundamental hypothesis is to design the scaffold to provide a biomimetic mechanical environment to withstand *in vivo* stress

[a]*Institute of Materials Research and Engineering (IMRE), 3 Research Link, Singapore 117602. E-mail: x-li@imre.a-star.edu.sg; Fax: +65 6872 7528; Tel: +65 6874 8421*
[b]*Division of Bioengineering, NUS, Singapore 119260*
[c]*Department of Materials Science & Engineering (DMSE), Faculty of Engineering, National University of Singapore (NUS), Singapore 117576*
[d]*Institute of Health and Biomedical Innovation, Queensland University of Technology (QUT), Brisbane, 4059, Australia*
[e]*Department of Mechanical Engineering, National University of Singapore (NUS), Singapore 117576. E-mail: mpegi@nus.edu.sg; Fax: +65 6779 1495; Tel: +65 9277 7343*

† Electronic supplementary information (ESI) available. See DOI: 10.1039/c1sm05793f

and loading.[8] Specifically, it was proposed that the implanted scaffold should match the stiffness and strength of native tissue,[6,7] which ranges from 50 to 500 MPa and 3 to 12 MPa for cancellous bone, respectively.[9,10]

Additive manufacturing (AM) technology, also known as rapid prototyping (RP), is a computer controlled fabrication process and holds the key for a generic solution in automating scaffolds production because of its consistency and high reproducibility. It has great potential over conventional manual-based fabrication techniques, as the scaffolds fabricated by AM are design dependent, whereas the scaffolds fabricated by conventional techniques are highly process dependent.[11] Poly(ε-caprolactone) (PCL) is a bioresorbable and thermoplastic aliphatic polyester, and has been used preferably to fabricate scaffolds with AM technology because it is easy to form at relatively low temperature and has good melt viscosity.[12–15] In order to increase the mechanical properties and bioactivity of these PCL scaffolds, pristine ceramic particles such as hydroxyapatite (HA) and tricalcium phosphate (TCP) have been mixed into the PCL matrix directly.[16–19]

Nevertheless, to date, only a slight improvement in compressive modulus and yield strength was achieved with PCL/ceramic composite scaffolds compared with those of PCL scaffolds. As an example, PCL/tricalcium phosphate (TCP) composite scaffolds exhibited a compressive modulus of 9.3 MPa and compressive yield strength of 3.1 MPa, while PCL scaffolds exhibited a compressive modulus of 2.7 MPa and compressive yield strength of 1.5 Mpa.[18] These PCL/TCP scaffolds are remarkably weak for cancellous bone tissue engineering. As reported recently in the review paper by Rezwan K. *et al.*, the limited improvement on mechanical properties of polymer/ceramic composite scaffolds is because of the relatively low interfacial bonding between ceramic filler and polymer matrix.[9] Another study has also demonstrated that effective stress transfer across the interface between polymer and ceramic filler is crucial for producing composite scaffolds with adequate mechanical properties.[20]

Good osteoconductive property is another crucial requirement of ideal scaffolds for bone tissue engineering.[7,21] Though the incorporated ceramic particles were supposed to improve the osteoconductive property of the composite scaffolds,[18] the limited exposure of ceramics on the composite scaffold surface diminishes this.[22] The limited exposure may be due to enveloping of ceramic particles by polymer during composite preparation and/or the scaffold fabrication process. Therefore, to improve the osteoconductive property of polymer/ceramic composite scaffolds, a layer of apatite coating on the scaffolds surface is considered as an effective approach. However, a previous study on melt extrusion based AM scaffolds coated with apatite did not find any promising result due to flaking of the thick apatite layer on the bars of scaffolds.[23] To reduce the flaking tendency a composite coating may be desirable. A recent study indicated that apatite/collagen composite coating has a significantly higher coating retention on titanium compared to pure apatite coating.[24]

Here, high performance additive manufactured PCL/TCP(Si) scaffolds have been developed for cancellous bone tissue engineering. Firstly, TCP was modified using 3-glycidoxypropyl trimethoxysilane (GPTMS) to enhance the interfacial bonding between TCP and PCL matrix. To ensure the formation of covalent bonding between TCP(Si) and PCL, the compounded PCL/TCP(Si) composites was annealed at 120 °C for 2 h. Melt extrusion based AM PCL/TCP(Si) scaffolds were then fabricated using an in-house screw extrusion system (SES) from the reinforced PCL/TCP(Si) composite. Secondly, carbonated hydroxyapatite (CHA)-gelatin composite was coated onto AM PCL/TCP(Si) scaffolds through a biomimetic co-precipitation process to improve their osteoconductive property. Studies on cell-scaffold interaction were carried out by culturing porcine bone marrow stromal cells (BMSCs) on the scaffolds and assessing proliferation, bone related gene and protein expression capabilities of the BMSCs. We hypothesized that such developed CHA-gelatin composite coated PCL/TCP(Si) scaffolds would provide not only adequate mechanical properties but also an excellent biocompatible environment to cells for better proliferation and osteogenic differentiation.

Results and discussions

PCL/TCP(Si) composite preparation and scaffolds fabrication

In order to prepare additive manufactured PCL/TCP scaffolds with adequate mechanical properties for cancellous bone tissue engineering, the interfacial bonding between PCL and TCP was enhanced by modifying TCP using GPTMS as a coupling agent. The main idea is that the epoxide group from GPTMS attached to TCP could react with the end groups of the PCL chain (OH and COOH) to form a covalent bond during melt-compounding and the followed annealing. Fig. 1 shows the schematic diagram of TCP modification as well as the covalent bond formation between TCP(Si) and PCL. First, hydroxyl groups were introduced onto TCP by stirring its suspension in a diluted phosphoric acid (2 wt%) for 2 h as reported previously.[25] Then, GPTMS was covalently bonded onto the surface of TCP *via* a condensation reaction with the introduced hydroxyl group on TCP. The successful modification of TCP was verified by X-ray photoelectron spectroscopy (XPS) and Fourier transform infrared spectroscopy (FTIR). As shown in Fig. 2, while only calcium, phosphorous and oxygen are detected on the surface of the non-treated TCP using XPS, additional silicon peaks (Si(2p): 99.8 eV; and Si(2s): 149.7 eV) from GPTMS are observed in the XPS spectrum of TCP(Si), confirming the presence of GPTMS on TCP. In the FTIR spectrum of TCP(Si) (Fig. 3b), observation of an additional characteristic epoxide band at 873 cm^{-1} in

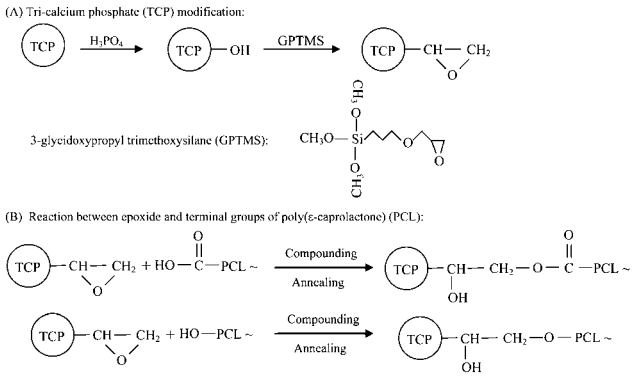

Fig. 1 Schematic diagram of TCP modification and PCL/TCP(Si) composite preparation.

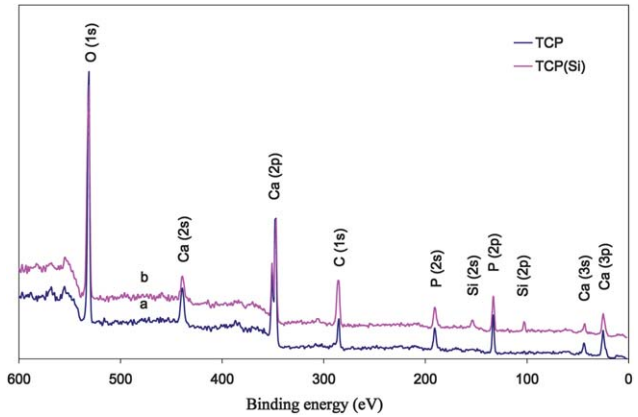

Fig. 2 XPS spectra of (a) TCP and (b) TCP(Si).

comparison to that of TCP also confirms the presence of GPTMS on TCP(Si). TCP(Si) with varying concentration of GPTMS was synthesized to study the influence of GPTMS content on the mechanical property of PCL/TCP(Si) scaffolds.

The synthesized TCP(Si) was suspended in acetone and mixed into PCL acetone solution by homogenizing at high speed. After evaporating off acetone using a rotary evaporator, the PCL/TCP (Si) composite was melt-compounded at 120 °C for 20 min followed by annealing at 120 °C for 2 h to facilitate the formation of covalent bonds between epoxide from TCP(Si) and OH or COOH from PCL. A similar chemical reaction has been reported previously.[26,27]

Additive manufactured PCL/TCP(Si) scaffolds (Fig. S1†) were fabricated from the above synthesized PCL/TCP(Si) composite using an in-house screw extrusion system (SES). SES is a potential melt extrusion based AM technology and has been used to fabricate scaffolds with specifically tailored pore geometry and architectural pattern.[17] In this study, the fabricated scaffolds were 100% interconnected with a pore size of 750–950 μm and an overall porosity of 65%. Additive manufactured PCL/TCP scaffolds with the same dimension were also fabricated as controls.

The compressive modulus and yield strength of PCL/TCP(Si) scaffolds with varying content of GPTMS were measured by compression testing, and compared with those of PCL/TCP scaffold. As shown in Fig. 4, both compressive modulus and yield strength of PCL/TCP(Si) scaffolds are significantly higher than those of the PCL/TCP scaffold, and PCL/TCP(Si) scaffold with 10 wt% of GPTMS with respect to TCP exhibits the maxima compressive modulus of 82.6 MPa and a compressive yield strength of 4.0 MPa, which are 6.0 and 2.3 times of those of PCL/TCP scaffolds, respectively. A slight reduction in the modulus at GPTMS of 15 wt% or higher might be due to formation of a thin layer of polysiloxane condensed from GPTMS on the surface of TCP, which works as a plasticizer to reduce the modulus. It should be noted that both the compressive modulus and yield strength of PCL/TCP(Si) scaffolds with a GPTMS content higher than 5 wt% fall in the lower range of mechanical properties of cancellous bone (50 to 500 MPa and 3 to 12 MPa), whereas the PCL/TCP scaffolds are remarkably weaker. As PCL/TCP(Si) scaffold with 10 wt% of GPTMS with respect to TCP exhibits the best mechanical properties, it has been chosen for coating and *in vitro* evaluation, and is denoted as PCL/TCP(Si).

PCL is a semi-crystalline polymer, and the crystallinity degree of PCL in PCL/TCP and PCL/TCP(Si) with various GPTMS content were measured using differential scanning calorimeter (DSC) and the results were listed in Table 1. It was found that the crystallinity degree of PCL in PCL/TCP(Si) with various GPTMS content is much higher than that in PCL/TCP. This may be due to the enhanced interfacial bonding between TCP(Si) and PCL, leading to higher nucleating efficiency of TCP(Si) for the

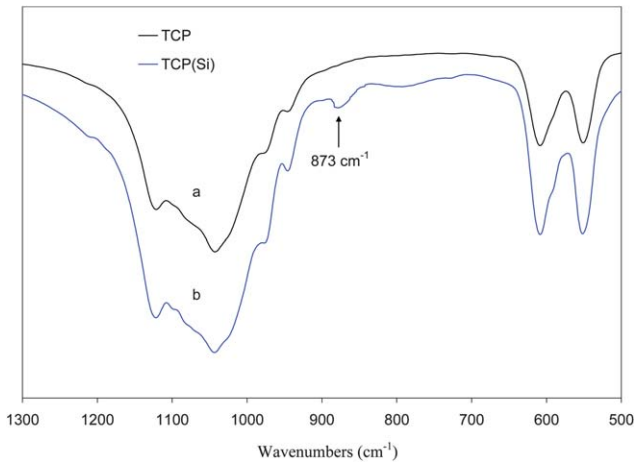

Fig. 3 FTIR spectra of (a) TCP and (b) TCP(Si).

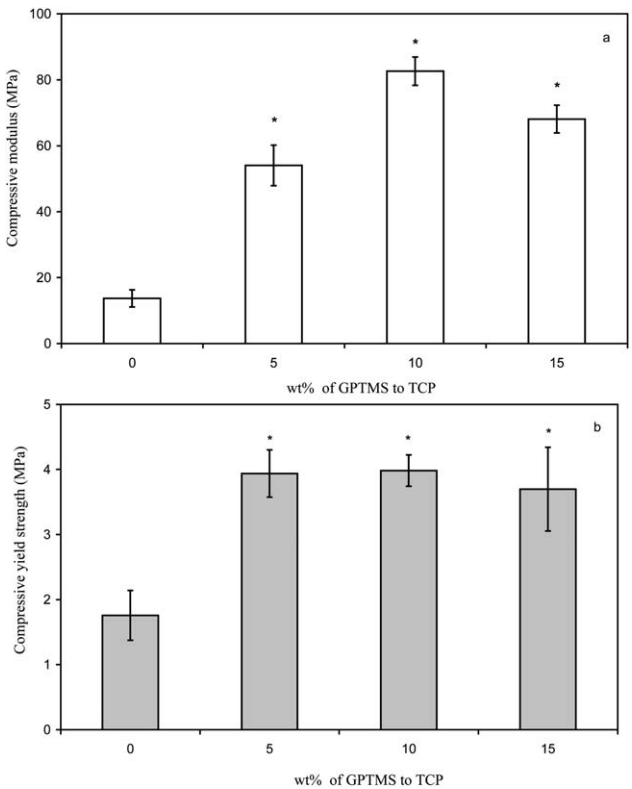

Fig. 4 Compressive modulus (a) and compressive yield strength (b) of PCL/TCP and PCL/TCP(Si) scaffolds with various content of GPTMS on TCP (* indicates $p < 0.05$). 0 wt% of GPTMS to TCP refers to PCL/TCP.

Table 1 Thermal property of PCL/TCP(Si) composites determined by DSC

wt% of GPTMS to TCP	Melting T_m/°C	Crystallinity (%)
0	55.3	39.9
5	55.0	47.2
10	55.1	47.7
15	54.8	46.4

crystallization of PCL. This increase in the crystallinity degree is correlated with the enhancement in compressive modulus and yield strength.[28] But, the melting temperature seemed to be independent of the introduction of GPTMS.

Biomimetic CHA-gelatin composite coating on PCL/TCP(Si) scaffolds

Natural bone extracellular matrix (ECM) mainly consists of collagen and carbonated hydroxyapatite (CHA) composite.[29] In comparison to collagen, collagen-based gelatin has almost an identical composition and is much cheaper.[30] Since gelatin is denatured, it also overcomes the possible risk of immunogenicity and pathogen transmission associated with collagen. Hence, to improve the osteoconductive property of the additive manufactured PCL/TCP(Si) scaffolds, a CHA-gelatin composite was coated onto the scaffolds through a biomimetic co-precipitation process.

In order to facilitate biomimetic mineralization on the surface of the PCL/TCP(Si) scaffolds, $CaHPO_4$ was coated onto their struts first as a nucleation site for CHA coating or CHA-gelatin composite coating by dipping NaOH treated scaffolds alternately in calcium chloride and potassium phosphate solutions, as reported previously.[31] To prepare CHA-gelatin composite coated PCL/TCP(Si) scaffolds (PCL/TCP(Si)-CHA-gelatin), the $CaHPO_4$ coated PCL/TCP(Si) scaffolds were then immersed into gelatin acetic acid solution followed by simultaneously adding dropwise $CaCl_2$ and H_3PO_4 aqueous solutions, and further dropwise addition of Na_2CO_3 aqueous solution according to the approach for CHA-gelatin composite preparation as reported previously.[32] The carboxyl and amine groups present in the gelatin may become charged groups under the coating conditions, such as COO^- and NH_3^+, which promote CHA-gelatin composite formation. It should be noted that the CHA-gelatin composite coating is free of chemical cross-linking with gelatin. Thus, this approach avoids the risk of toxicity caused by chemicals employed for cross-linking gelatin in other approaches.[33,34] By the biomimetic approach described here, mineralization can be achieved in just a few hours, whereas conventional mineralization may take a few weeks.[35,36] Moreover, unlike the conventional biomimetic approach, the developed process does not demand a constant pH to maintain supersaturation for apatite crystal growth. PCL/TCP(Si) scaffolds coated with CHA alone (PCL/TCP(Si)-CHA) were also prepared following the same process without adding gelatin to study the influence of gelatin incorporation on the osteoconductive property of the scaffolds.

The surface morphology of the PCL/TCP(Si), PCL/TCP(Si)-CHA and PCL/TCP(Si)-CHA-gelatin scaffolds was characterized by using SEM. As shown in Fig. 5, while the PCL/TCP(Si) scaffolds exhibits a smooth surface, both the PCL/TCP(Si)-CHA and PCL/TCP(Si)-CHA-gelatin scaffolds exhibit rough surfaces with uniform coating throughout the whole surface. The CHA coating looks like globular apatite (Fig. 5b) and the CHA-gelatin composite coating looks like plate-like apatite (Fig. 5c). The morphology difference between the CHA coating and CHA-gelatin composite coating could be due to the presence of gelatin in the biomimetic co-precipitation for the CHA-gelatin composite coating, as it is known that adsorption of protein on the mineral surface can alter the nucleation and growth of crystals in biomineralization.[37] The thickness of the CHA coating and the CHA-gelatin composite coating are measured as 702 ± 56 nm and 635 ± 119 nm from their cross-section SEM images, respectively (Fig. S2†).

Compression testing of the CHA and CHA-gelatin coated scaffolds was also conducted and the results demonstrated that coating does not influence the mechanical properties of the PCL/TCP(Si) scaffolds (Fig. S3†).

The chemical structure of the coating was studied by using XPS. No characteristic peaks of calcium and phosphorous detected in the XPS spectrum of PCL/TCP(Si) scaffolds (Fig. 6a) implies that ceramic particles of TCP(Si) are covered by PCL during composite preparation and/or scaffold fabrication as reported previously.[22] In contrast, characteristic peaks of calcium and phosphate are observed in the XPS spectra of both PCL/TCP(Si)-CHA and PCL/TCP(Si)-CHA-gelatin scaffolds. Moreover, a nitrogen peak is detected in the XPS spectrum of PCL/TCP(Si)-CHA-gelatin scaffolds (Fig. 6d). All these confirm the successful formation of CHA and CHA-gelatin coating on the strut surface of PCL/TCP(Si) scaffolds.

In vitro cells response

The cell-scaffold interaction is crucial for tissue engineering, and an ideal scaffold provides a suitable environment for cells to proliferate and differentiate. BMSCs have self-renewal

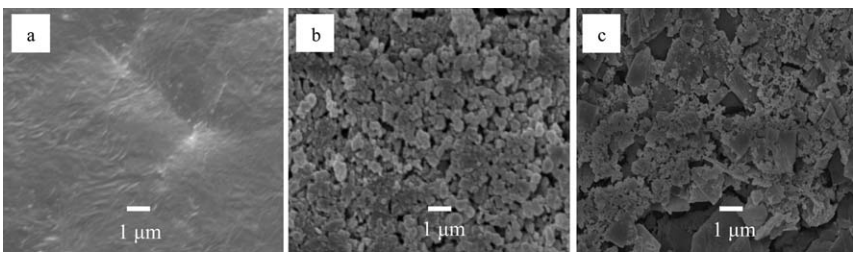

Fig. 5 SEM images of (a) PCL/TCP(Si), (b) PCL/TCP(Si)-CHA and (c) PCL/TCP(Si)-CHA-gelatin scaffolds.

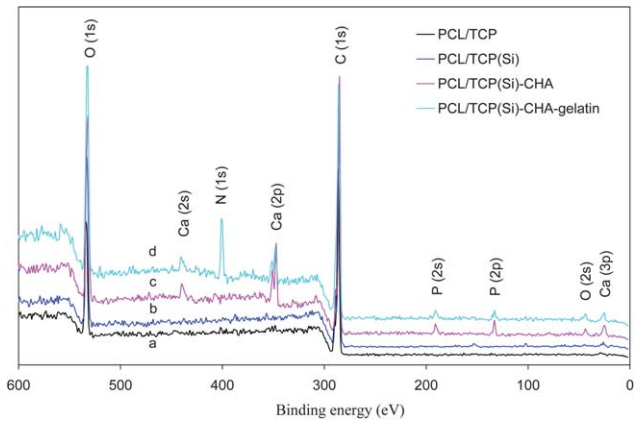

Fig. 6 XPS spectra of (a) PCL/TCP, (b) PCL/TCP(Si), (c) PCL/TCP (Si)-CHA and (d) PCL/TCP(Si)-CHA-gelatin scaffolds.

capability, multilineage differentiation potential and a similar prospect as embryonic stem cells, but they are less related with ethical issues and tumorigenesis risks.[38] Therefore, BMSCs have been widely employed for *in vitro* studies of bone formation and evaluating the biocompatibility of a newly developed material for bone tissue engineering.[38–40] In this study, the proliferative and osteoconductive properties of the prepared scaffolds are evaluated by observing BMSCs morphology, proliferation, and gene and protein expression.

Fig. 7 shows the SEM images of BMSCs cultured on PCL/TCP, PCL/TCP(Si), PCL/TCP(Si)-CHA and PCL/TCP(Si)-CHA-gelatin scaffolds at day 7. Highest level of cells and cell-sheet accumulation were observed on PCL/TCP(Si)-CHA-gelatin scaffolds among all the scaffolds. Moreover, from the overview image of the PCL/TCP(Si)-CHA-gelatin scaffolds it can be seen that tissue bridges have started to form (indicated by arrow in Fig. S4†). On the other hand, for both PCL/TCP and PCL/TCP (Si) scaffolds the cells spread in a comparatively limited manner.

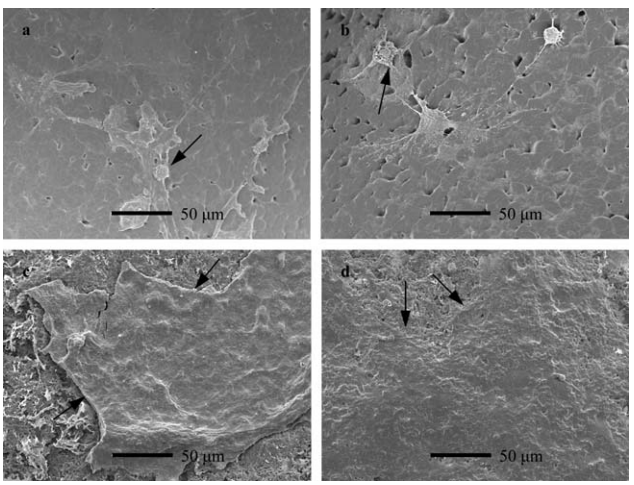

Fig. 7 SEM images of cell-scaffold construct of (a) PCL/TCP, (b) PCL/TCP(Si), (c) PCL/TCP(Si)-CHA and (d) PCL/TCP(Si)-CHA-gelatin scaffolds at day 7. The arrow shows the cells and/or cell-sheet accumulation that have spread on the surface of the scaffolds.

Fig. 8 shows the confocal laser microscopy image of BMSCs cultured on PCL/TCP, PCL/TCP(Si), PCL/TCP(Si)-CHA and PCL/TCP(Si)-CHA-gelatin scaffolds at different culture times. At day 7, BMSCs stretched well over the struts and distributed uniformly in PCL/TCP(Si)-CHA and PCL/TCP(Si)-CHA-gelatin scaffolds, while qualitatively fewer BMSCs were observed in non-coated PCL/TCP and PCL/TCP(Si) scaffolds. At day 10, PCL/TCP(Si)-CHA-gelatin scaffolds exhibited tissue bridges between the struts (Fig. 9) as well as the most uniform distribution of viable cells among all the scaffold groups (Fig. 8). In contrast, at day 10, the BMSCs seeded in PCL/TCP and PCL/TCP(Si) scaffolds were predominantly in a round shape. It should be noted that our developed thin CHA-gelatin composite coating did not show any flaking tendency during cell culture as opposed to previous study,[23] demonstrating excellent adhesion of the biomimetic composite coating to the scaffolds.

Fig. 10 shows the proliferation of BMSCs in the cell-scaffold constructs studied by PicoGreen® assay. At all the time points, coated PCL/TCP(Si) scaffolds exhibit a higher amount of DNA in comparison to non-coated PCL/TCP and PCL/TCP(Si) scaffolds. At day 7, PCL/TCP(Si)-CHA-gelatin scaffolds exhibit significantly higher amounts of DNA in comparison to non-coated PCL/TCP and PCL/TCP(Si) scaffolds. At day 10, both PCL/TCP(Si)-CHA and PCL/TCP(Si)-CHA-gelatin scaffolds exhibit significantly higher amounts of DNA in comparison to non-coated PCL/TCP and PCL/TCP(Si) scaffolds, and the significantly highest amount of DNA content is exhibited by PCL/TCP(Si)-CHA-gelatin scaffolds among all the scaffolds, with a 1.4 and 2.0 times higher value than that of PCL/TCP(Si)-CHA and PCL/TCP(Si) scaffolds, respectively. These findings signify the highest level of BMSCs proliferation on PCL/TCP (Si)-CHA-gelatin scaffolds among all the scaffold groups, which could be due to the presence of gelatin in CHA-gelatin composite coating. Gelatin is recognized to promote cell proliferation.[41] In addition, PCL/TCP and PCL/TCP(Si) scaffolds exhibited an almost similar amount of DNA content for all the time points. This demonstrates that PCL/TCP and PCL/TCP(Si) scaffolds posses almost the same level of biocompatibility, indicating GPTMS modification on TCP does not lead to any detrimental effect on BMSCs activity as reported previously on the biocompatibility of silane treated surface.[42–44]

The differentiation of BMSCs in the cell-scaffold constructs was studied by RT-PCR analysis. The quantitative RT-PCR analysis (Fig. 11) revealed that at day 17, PCL/TCP(Si)-CHA-gelatin and PCL/TCP(Si)-CHA scaffolds have 6.2 and 3.8 times higher expression levels of Core binding factor α1 (Cbfa1) than that of PCL/TCP(Si) scaffolds, respectively. At day 24, which is a later time point, the Cbfa1 expression levels of PCL/TCP(Si)-CHA-gelatin and PCL/TCP(Si)-CHA scaffolds were 1.4 and 4.3 times higher than that of PCL/TCP(Si) scaffolds, respectively. Cbfa1 is considered as an important transcription factor for the commitment of multipotent mesenchymal cells into the osteoblastic lineage by triggering the gene expression of bone matrix proteins.[44,45] Cbfa1 retains the osteoblastic cells at an immature stage by hampering the transition of osteoblasts to osteocytes. Generally, the expression of Cbfa1 is first noticed in preosteoblasts, and up regulated in immature osteoblasts, but down regulated in mature osteoblasts.[45,46] Cbfa1 is also involved in regulating bone phenotypic genes such as osteocalcin (OCN),

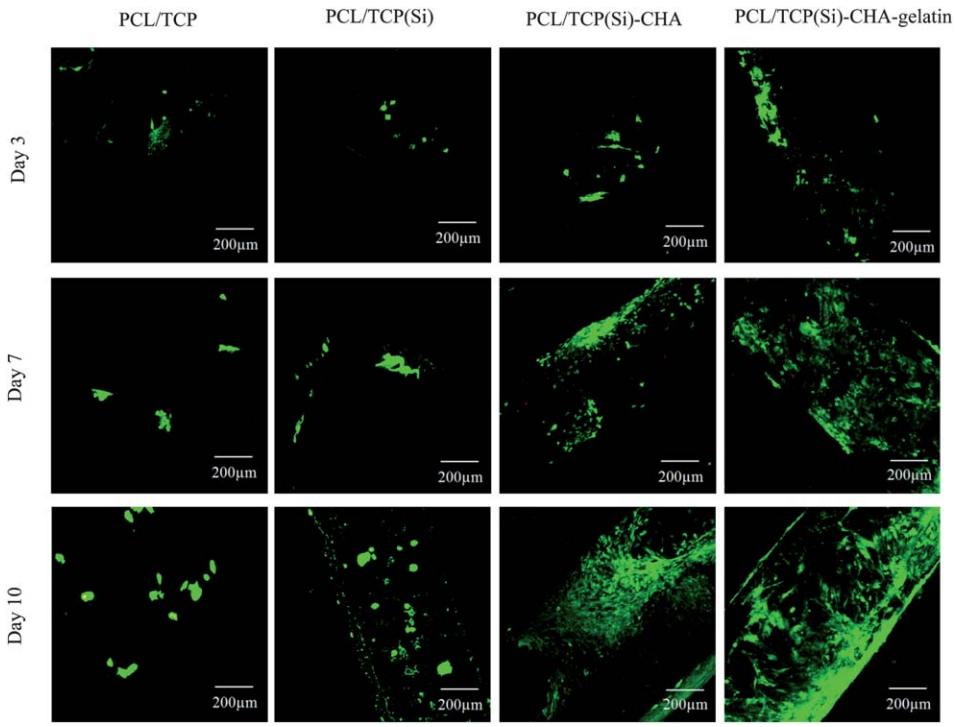

Fig. 8 Confocal laser microscopy with depth projection images reconstructed from multiple horizontal images, showing 3D distribution of cells within the scaffolds of PCL/TCP, PCL/TCP(Si), PCL/TCP(Si)-CHA and PCL/TCP(Si)-CHA-gelatin scaffolds.

one of the terminal differentiation markers.[45,47,48] It can be seen from Fig. 11, from day 17 to day 24, OCN increases from 4.2 times higher to 25.2 times higher for PCL/TCP(Si)-CHA-gelatin scaffolds than that of the PCL/TCP(Si) scaffolds, while the Cbfa1 decreases from 6.2 times higher to 1.4 times higher. Expression of collagen I (Col1) showed slightly basal expression levels for PCL/TCP(Si)-CHA-gelatin and PCL/TCP(Si)-CHA scaffolds compared to PCL/TCP(Si). Though the reason behind this phenomenon is not clear yet, basal regulation of Col1 expression of marrow stromal cells (MSC) on hydroxyapatite after day 10 has also been reported previously.[49,50] From the above results it can be concluded that though cells express almost similar amount of Col1 transcription, they show significantly more expression of mature ostoegenic gene OCN for coated scaffolds, which eventually indicate that the cells on the coated PCL/TCP(Si) scaffolds are more in the osteogenic lineage.

To analyze the extracts of protein formed on cell-scaffold constructs, western blotting was carried out after BMSCs were cultured for 31 days. Osteonectin (ON) is an important non-collagen calcium binding glycoprotein related to mineralisation at the early stage of bone formation secreted by osteoblasts. As can be seen from Fig. 12, the expression of ON is 2.5 and 2.2 times higher on PCL/TCP(Si)-CHA-gelatin and PCL/TCP(Si)-CHA scaffolds

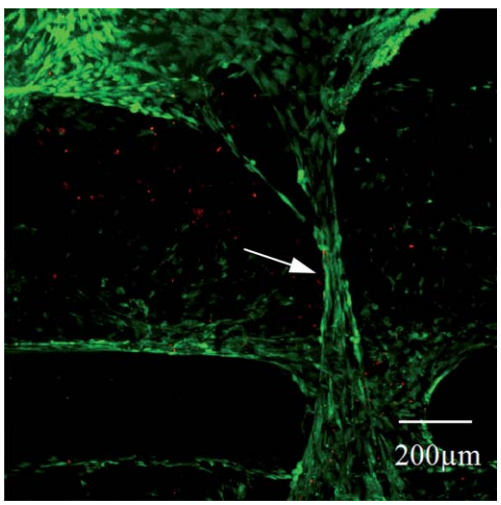

Fig. 9 Confocal laser microscopy image of PCL/TCP(Si)-CHA-gelatin scaffolds at day 10, showing a tissue bridge as indicated by the arrow.

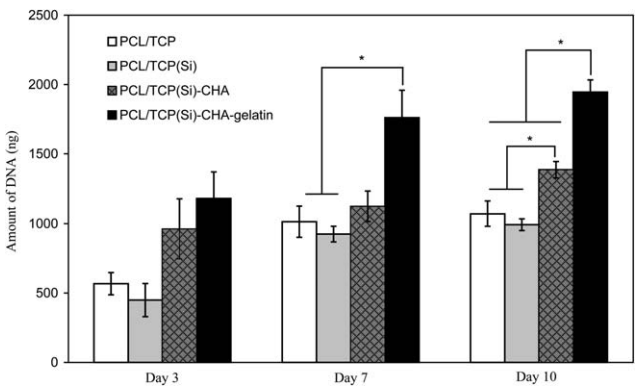

Fig. 10 PicoGreen® DNA quantification results of BMSCs cultured on PCL/TCP, PCL/TCP(Si), PCL/TCP(Si)-CHA and PCL/TCP(Si)-CHA-gelatin scaffolds (* indicates $p < 0.05$).

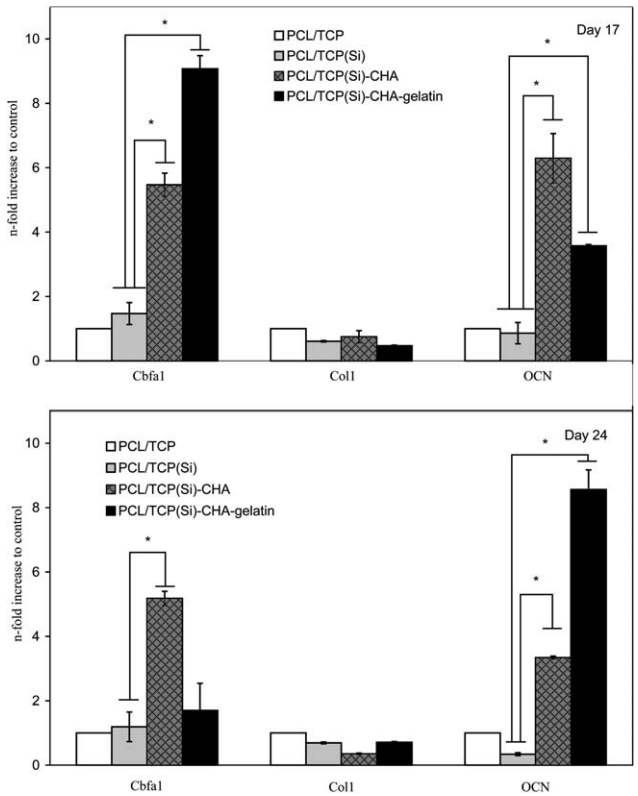

Fig. 11 mRNA expression of Cbfa1, collagen I (Col1) and osteocalcin (OCN) of BMSCs cultured for 17 days and 24 days on PCL/TCP, PCL/TCP(Si), PCL/TCP(Si)-CHA and PCL/TCP(Si)-CHA-gelatin scaffolds (* indicates $p < 0.05$).

compared to that on PCL/TCP(Si) scaffolds, respectively. OCN is a bone-specific glycoprotein found abundantly in bone and dentin. This non-collagenous protein is secreted by osteoblasts. It is known to promote calcification of the bone matrix, and has been studied as a late marker for osteogenic differentiation and osteoblast maturation[38,45,51] The expression of OCN is 1.2 and 1.3 times higher on PCL/TCP(Si)-CHA-gelatin and PCL/TCP(Si)-CHA scaffolds than that on PCL/TCP(Si) scaffolds, respectively.

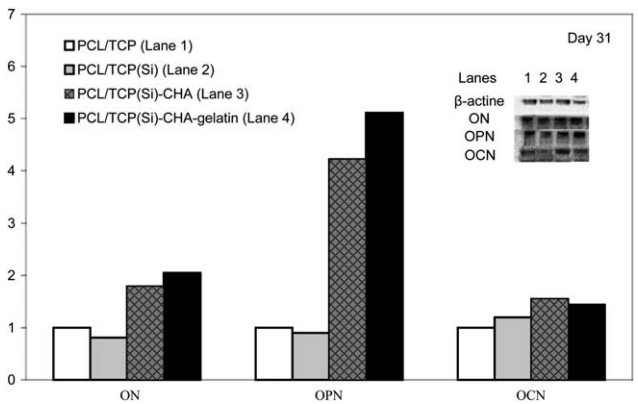

Fig. 12 Protein extracts of osteonectin (ON), osteopontin (OPN) and osteocalcin (OCN) from cell-scaffold constructs after BMSCs were cultured for 31 days on PCL/TCP, PCL/TCP(Si), PCL/TCP(Si)-CHA and PCL/TCP(Si)-CHA-gelatin scaffolds.

Osteopontin (OPN) is another mineral-binding protein found in bone extracellular matrix and is associated with cell attachment, proliferation, and biomineralization of extracellular matrix into bone. Its expression exhibits the commitment of BMSCs to osteogenic differentiation.[51] A significantly higher level (5.7 times) of OPN expression was observed on PCL/TCP(Si)-CHA-gelatin scaffolds compared to that on PCL/TCP(Si) scaffolds. At the same time, PCL/TCP(Si)-CHA scaffolds showed 4.7 times higher OPN expression compared to PCL/TCP(Si) scaffolds. Fig. 12 also showed a higher amount of ON and OPN expression on PCL/TCP (Si)-CHA-gelatin scaffolds than that on PCL/TCP(Si)-CHA scaffolds. Stimulation of osteogenic differentiation of BMSCs on PCL/TCP(Si)-CHA-gelatin scaffolds may be due to the presence of gelatin in the CHA-gelatin composite coating.[52] A previous study on collagen and HA showed that the addition of collagen to hydroxyapatite implants can enhance both phagocytotic and osteogenic processes.[53] These results suggest that CHA-gelatin composite coating on PCL/TCP(Si) scaffolds improved the proliferation and osteoconductive capability of the scaffolds significantly.

Conclusions

Additive manufactured PCL/TCP(Si) scaffolds with enhanced mechanical and osteoconductive properties have been successfully prepared. TCP was modified by using GPTMS and the modified TCP has been incorporated into PCL to form a reinforced PCL/TCP(Si) composite through homogenization followed by melt compounding and annealing at 120 °C for 2 h. The successful modification of TCP was verified by XPS and FTIR analysis. Additive manufactured PCL/TCP(Si) scaffolds with 100% interconnectivity and 65% porosity were fabricated using an in-house SES. The PCL/TCP(Si) scaffolds showed a 6.0 times higher compressive modulus and 2.3 times higher compressive yield strength than those of PCL/TCP scaffolds and eventually match with the lower range mechanical properties of cancellous bone. The osteoconductive property of the PCL/TCP(Si) scaffolds was improved by coating with CHA-gelatin composite *via* a biomimetic co-precipitation process, which was verified by XPS analysis. SEM and confocal images demonstrated the highest level of cells and cell-sheet accumulation with the most uniform distribution on PCL/TCP(Si)-CHA-gelatin scaffolds, compared to all other scaffolds. The proliferation rate of BMSCs on CHA-gelatin composite coated PCL/TCP(Si) scaffolds were 2.0 and 1.4 times higher than that of PCL/TCP(Si) and CHA coated PCL/TCP(Si) scaffolds, respectively, by day 10. *In vitro* RT-PCR and western blotting testing showed the highest level of osteoconductive property on PCL/TCP(Si)-CHA-gelatin compared to all other scaffolds. Moreover, no negative effects of GPTMS modification was noticed. This study clearly extends the potential of melt extrusion based additive manufactured composite scaffolds for bone tissue engineering applications.

Experimental

Materials

Poly(ε-caprolactone) (PCL) (M_n: 80,000), 3-glycidoxypropyl trimethoxysilane (GPTMS), gelatin (type A, from porcine skin), acetic acid (CH_3COOH), calcium chloride ($CaCl_2$), potassium

hydrophosphate (K_2HPO_4), phosphoric acid (H_3PO_4, 85% solution in water), sodium carbonate (Na_2CO_3) and sodium hydroxide (NaOH) were purchased from Sigma-Aldrich, Singapore. Tri-calcium phosphate (TCP) was purchased from Progentix, The Netherlands.

Synthesis of PCL/TCP(Si)

Surface activation of TCP was carried out by stirring TCP in 2% phosphoric acid (1 : 2 w/w) at room temperature for 2 h followed by sonicating for 5 min.[25] The surface activated TCP was washed first with distilled water for 3 times to remove free phosphoric acid and then with acetone for 3 times to remove water, and suspended in actone. GPTMS was then added into TCP acetone suspension and refluxed at 75 °C for 24 h. GPTMS modified TCP (TCP(Si)) was collected through filtration followed by a thorough wash with acetone to remove free GPTMS. The TCP(Si) was incorporated into PCL through homogenizing PCL/TCP(Si) acetone solution at 8000 rpm for 15 min. After evaporating off acetone, the homogenized composite was vacuum dried at 50 °C for 1 week. Finally, PCL/TCP(Si) composite was melt compounded at 120 °C for 20 min and annealed at 120 °C for 2 h.

Fabrication of the PCL/TCP(Si) scaffolds by SES

Additive manufactured PCL/TCP(Si) composite scaffolds were fabricated using an in-house screw extrusion system (SES) with screw rotational speed of 25 rpm and nozzle diameter of 0.4 mm at a processing temperature of 85 °C. The dispensing speed of the machine was 4 mm s^{-1} and the center to center distance of the scaffold struts was set to 1.5 mm. Each layer of the scaffolds was fabricated with the designed pattern of 0°/60°/120° orientation. The size of the scaffolds used for mechanical test was 5 mm × 5 mm × 8 mm and for the cell culture was 5 mm × 5 mm × 3.5 mm. The reason of choosing relatively lower height scaffolds is to use the available resources efficiently. PCL/TCP scaffolds were also fabricated as control.

Surface coating on PCL/TCP(Si) scaffolds

As PCL/TCP(Si) scaffold with 10 wt% of GPTMS with respect to TCP exhibits the best mechanical properties; therefore, it has been used for coating and *in vitro* evaluation and is denoted as PCL/TCP(Si). The PCL/TCP(Si) scaffolds were immersed in aqueous NaOH solution (10 ml, 5 M) at room temperature for 12 h followed by thorough washing with de-ionized water. The NaOH treated scaffolds were dipped into calcium chloride solution and potassium hydrophosphate solution alternately to achieve $CaHPO_4$ coating.[31] In detail, the scaffolds were initially dipped in $CaCl_2$ aqueous solutions (20 mL, 0.2 M) for 10 min, and then dipped in de-ionized water for 5 s followed by air drying for 3 min. The treated scaffolds were subsequently dipped in K_2HPO_4 aqueous solutions (20 mL, 0.2 M) for 10 min, and then dipped in de-ionized water for 5 s followed by air drying for 3 min. The whole process was repeated three times.

The $CaHPO_4$ coated PCL/TCP(Si) scaffolds were immersed into CH_3COOH (20 ml, 0.1 M), and then $CaCl_2$ (10 ml, 0.1 M) and H_3PO_4 (6 ml, 0.1 M) with a Ca/P ratio of 1.66 were gradually added through respective syringe pumps under stirring. After 30 min of stirring, Na_2CO_3 (18 ml, 0.1 M) with the molar ratio of CO_3^{2-}/PO_4^{3-} of 3 was gradually added. The mixture was further stirred for another 30 min and then titrated to pH 9 using NaOH (0.1 M). After the solution was aged for 3 h, the CHA coated PCL/TCP(Si) scaffolds (PCL/TCP(Si)-CHA) were taken out, washed with de-ionized water and freeze dried.

For preparing CHA-gelatin composite coated PCL/TCP(Si) scaffolds, $CaHPO_4$ coated PCL/TCP(Si) scaffolds were immersed into CH_3COOH (10 mL, 0.1 M) solution dissolved with gelatin (40 mg). Then, CHA-gelatin composite coated PCL/TCP(Si) (PCL/TCP(Si)-CHA-gelatin) scaffolds were achieved by adding $CaCl_2$, H_3PO_4, Na_2CO_3 and NaOH following the same process as that of CHA coating described above.

Characterization

The surface chemical structure of TCP(Si) and PCL/TCP(Si) scaffolds were characterized by XPS (Thetaprobe from Thermo Scientific), using a source of monochromated Al K_α (1486.6 eV) along with a flood gun for surface charge compensation (energy 2 eV, emission current 100 mA). The detector was set at standard lens mode CAE (contact analyzer energy) and passed energy for survey spectra is 200 eV and 40 eV for high resolution spectra. Data analysis was done using the Avantage software. FTIR spectra of TCP and TCP(Si) minced into the KBr pallet were recorded on a Bio-Rad 165 FT-IR spectrophotometer; 64 scans were signal-averaged with a resolution of 2 cm^{-1} at room temperature. Differential scanning calorimetry (DSC) measurements were performed using a TA Instruments 2920 differential scanning calorimeter equipped with an auto-cooling accessory and calibrated using indium. The following protocol was used for each sample: heating from room temperature to 120 °C at 20 °C min^{-1}, holding at 120 °C for 2 min, cooling from 120 to −30 °C at 5 °C min^{-1}, and finally reheating from −30 to 170 °C at 5 °C min^{-1}. Data were collected during the second heating run. The degree of crystallinity was calculated according to the following equation:

Crystallinity (%) = $(\Delta H_m/(80\%)/\Delta H_m^\circ) \times 100\%$; where H_m is the melting enthalpy (J g^{-1}) of composite; 80% is the weight percentrage of PCL in the composite and ΔH_m° (139.5 J g^{-1}) is the melting enthalpy of 100% crystalline PCL.[54]

Compressive modulus and compressive yield strength of the scaffolds were measured using an Instron 4502 uniaxial testing system with 5 kN load cell. All scaffolds had the size of 5 mm × 5 mm × 8 mm and 0°/60°/120° lay down patterns. Ten scaffolds were tested from each group and measurements were reported as mean ± standard deviation.

The surface morphology of the scaffolds was studied with a Quanta 200F field emission scanning electron microscope (FESEM) at a beam intensity of 10 kV after gold sputtering using a JFC-1200 fine sputter coater.

Cell seeding on scaffolds

Tissue culture media Dulbecco's modified Eagle's medium (DMEM), fetal bovine serum (FBS) and *penicillin*-streptomycin (pen-strep) were purchased from Gibco. Trypsin-EDTA was purchased from Thermo Scientific Hyclone.

Cryo-preserved porcine BMSCs (passage 2) were isolated from the iliac crest of pigs and expanded in T75 tissue culture flasks in

Table 2 Forward primers and reverse primers used in RT-PCR

Gene ID	Forward Primer	Reverse Primer
GAPDH	GCTTTGCCCCGCGATCTAATGTTC	GCCAAATCCGTTCACTCCGACCTT
CBFA1	GAGGAACCGTTTCAGCTTACTG	CGTTAACCAATGGCA CGA G
COL1	CCAAGAGGAGGGCCAAGAAGAAGG	GGGGCAGACGGGGCAGCACTC
OCN	TCAACCCCGACT GCGACGAG	TTGGAGCAGCTG GGATGATGG

DMEM supplemented with 10% FBS and 1% antibiotics until getting sufficient cells (not beyond passage 4). Medium was changed twice a week and cells were detached by trypsin-EDTA and transferred into fresh culture flasks at a ratio of 1 : 3 upon reaching confluence. Cultures were incubated at 37 °C in a humidified atmosphere with 5% CO_2.

To sterilize the scaffolds, first the scaffolds were treated with ethanol (70%) for 30 min and then treated under UV light for 30 min followed by drying in sterile condition at room temperature for 2 h. Four groups of scaffolds were prepared namely, PCL/TCP, PCL/TCP(Si), PCL/TCP(Si)-CHA and PCL/TCP(Si)-CHA-gelatin, and BMSCs (1.8×10^5 cells) were added onto each scaffold. The cell-scaffold constructs were cultured up to 10 days in growth medium, and at specific time points cell-scaffold constructs were assessed and observed for proliferation. For osteogenic induction, after 10 days of culture in growth medium, an osteogenic cocktail of dexamethasome (10 nM), ascorbic acid (50 μM) and β-glycerolphosphate (10 mM) (Sigma) was added. The cell-scaffold constructs were cultured further for 28 days post induction and samples were assessed at definite time points for gene and protein expressions.

Morphology of the cell-scaffold constructs

SEM and confocal laser microscopy were used to assess cell morphology, viability and attachment *in vitro*. BMSCs were stained with fluorescein diacetate (FDA) (2 μg ml^{-1}) (Molecular probes), which stains the cytoplasm of the live cells with green fluorescence. During FDA staining samples were incubated at 37 °C for 15 min followed by rinsing with PBS. Samples were then counterstained with propidium iodide (PI) (5 μg mL^{-1}) (Molecular probes) to stain the nucleus of the dead cells with red fluorescence. During PI staining the samples were kept at room temperature for 2 min and then rinsed with PBS. Finally the samples were viewed under confocal laser microscope (IX 70, Olympus). Depth projection images were constructed from up to 25 horizontal image sections (12 μm each) through the stained cell-scaffold constructs using FV1000 Viewer (Ver.1.7a) software. After confocal imaging, cell-scaffold constructs were fixed in formalin (10%) overnight and then dehydrated through a series of graded ethanol solutions (5, 10, 20, 40, 60, 80, 90 and 100%), each for 10 min for dehydration. Finally, the samples were dried overnight at room temperature and were gold sputtered to observe under SEM at an accelerating voltage of 10 kV.

PicoGreen® assay

Proliferation of BMSCs in cultured cell-scaffold constructs were studied using the PicoGreen® assay as per manufacturer's protocol (Molecular Probes, PicoGreen dsDNA Quantitation kit). Total DNA from cells in the constructs were extracted *via* freeze-thaw cycles. DNA amount in the cell lysate were then assayed by mixing with DNA binding PicoGreen® dye followed by spectrophotometer quantisation.

Gene expression (Real-time RT-PCR)

At specified time points, the cell-scaffold constructs were lysed with Trizol (Invitrogen) and thoroughly vortexed. The samples in Trizol were stored at −80 °C until RNA isolation. Total RNA was isolated using the RNeasy Mini Kit (Qiagen) with Rnase-Free DNase (Qiagen) according to the manufacturer's protocol.

Reverse transcription was performed with the QuantiTect Reverse Transcriptase kit (Qiagen) to make the required cDNA. Quantitative PCR was performed for the quantification of gene expressions using the primers listed in Table 2 and QuantiTect SYBR Green PCR kit (Qiagen) Mx3000P *Real-Time PCR* System (Stratagene). Target genes were normalized against the GAPDH expression.

Western blot study (WB)

Protein extracts were harvested from the cell-scaffold constructs with ice-cold radioimmunoprecipitation assay (RIPA) buffer (Thermo Scientific). As the protein level from a single scaffold is usually too small for a gel run, the protein extracts were collected from 5 samples per group to get a more concentrated protein extract. The testing results are reported as an average of 5 samples. Protein lysates were purified and concentrated using NanoSep columns (Pall 3 K). Total protein quantity was quantified using microBCA assay (Pierce) as per manufacture's protocol. Proteins were denatured at 90 °C for 5 min, resolved by 10% SDS-PAGE (polyacrylamide gel electrophoresis) and transferred to nitrocellulose membranes (Bio-Rad). After blocking with 1% non-fat milk in tris-buffered saline (TBS) for 1 h, the membranes were then incubated for 1 h with primary antibodies: polyclonal rabbit-anti-human beta-actin (Delta Biolabs), osteonectin (ON), osteocalcin (OCN) (Santa Cruz) or osteopontin (OPN) (Abcam). The primary antibodies were diluted from 1 : 500 to 1 : 2000 in TBS with 0.1% Tween (TBST). After three washes with TBST, membranes were next incubated with rabbit anti-goat HRP-conjugated secondary IgG (Zymed) at 1 : 15,000 for 1 h, followed by another three washes with TBST. Immunoreactive bands were visualised and detected using the SuperSignal chemiluminescent reagent (Pierce) on the *VersaDoc* Imaging Systems (Bio-Rad). The intensities of the bands were quantitatively analyzed using densitometry (Quantity-*One*,

Bio-Rad). Target proteins were normalized against the β-actin expression.

Statistical analysis

All the data presented are expressed as mean ± standard deviation. An unpaired student's t-test was used to test the significance level of the data. Differences were considered statistically significant at $p < 0.05$.

Acknowledgements

Financial support from the A*STAR under the grant no. R 397 000 038 305 to this research is acknowledged.

References

1 H. Lohmann, G. Grass, C. Rangger and G. Mathiak, *Arch. Orthop. Trauma Surg.*, 2007, **127**, 345–348.
2 M. M. Stevens, *Mater. Today*, 2008, **11**, 18–25.
3 S. Gogolewski and K. Gorna, *J. Biomed. Mater. Res., Part A*, 2007, **80A**, 94–101.
4 S. J. Hollister, *Adv. Mater.*, 2009, **21**, 3330–3342.
5 M. J. Yaszemski, R. G. Payne, W. C. Hayes, R. Langer and A. G. Mikos, *Biomaterials*, 1996, **17**, 175–185.
6 D. W. Hutmacher, *J. Biomater. Sci., Polym. Ed.*, 2001, **12**, 107–124.
7 D. W. Hutmacher, *Biomaterials*, 2000, **21**, 2529–2543.
8 C. Y. Lin, N. Kikuchi and S. J. Hollister, *J. Biomech.*, 2004, **37**, 623–636.
9 K. Rezwan, Q. Z. Chen, J. J. Blaker and A. R. Boccaccini, *Biomaterials*, 2006, **27**, 3413–3431.
10 R. W. Goulet, S. A. Goldstein, M. J. Ciarelli, J. L. Kuhn, M. B. Brown and L. A. Feldkamp, *J. Biomech.*, 1994, **27**, 375–389.
11 K. F. Leong, C. M. Cheah and C. K. Chua, *Biomaterials*, 2003, **24**, 2363–2378.
12 M. A. Woodruff and D. W. Hutmacher, *Prog. Polym. Sci.*, 2010, **35**, 1217–1256.
13 D. W. Hutmacher, T. Schantz, I. Zein, K. W. Ng, S. H. Teoh and K. C. Tan, *J. Biomed. Mater. Res.*, 2001, **55**, 203–216.
14 M. Endres, D. W. Hutmacher, A. J. Salgado, C. Kaps, J. Ringe, R. L. Reis, M. Sittinger, A. Brandwood and J. T. Schantz, *Tissue Eng.*, 2003, **9**, 689–702.
15 J. T. Schantz, D. W. Hutmacher, C. X. F. Lam, M. Brinkmann, K. M. Wong, T. C. Lim, N. Chou, R. E. Guldberg and S. H. Teoh, *Tissue Eng.*, 2003, **9**, S127–S139.
16 F. Wang, L. Shor, A. Darling, S. Khalil, W. Sun, S. Guceri and A. Lau, *Rapid Prototyping Journal*, 2004, **10**, 42–49.
17 L. Shor, S. Guceri, X. J. Wen, M. Gandhi and W. Sun, *Biomaterials*, 2007, **28**, 5291–5297.
18 Y. F. Zhou, D. W. Hutmacher, S. L. Varawan and T. M. Lim, *Polym. Int.*, 2007, **56**, 333–342.
19 J. D. Kretlow and A. G. Mikos, *Tissue Eng.*, 2007, **13**, 927–938.
20 Y. F. Zhou, F. L. Chen, S. T. Ho, M. A. Woodruff, T. M. Lim and D. W. Hutmacher, *Biomaterials*, 2007, **28**, 814–824.
21 P. X. Ma, *Mater. Today*, 2004, **7**, 30–40.
22 D. Gupta, J. Venugopal, S. Mitra, V. R. G. Dev and S. Ramakrishna, *Biomaterials*, 2009, **30**, 2085–2094.
23 H. Chim, D. W. Hutmacher, A. M. Chou, A. L. Oliveira, R. L. Reis, T. C. Lim and J. T. Schantz, *Int. J. Oral Maxillofacial Surg.*, 2006, **35**, 928–934.
24 L. T. de Jonge, S. C. G. Leeuwenburgh, J. van den Beucken, J. te Riet, W. F. Daamen, J. G. C. Wolke, D. Scharnweber and J. A. Jansen, *Biomaterials*, 2010, **31**, 2461–2469.
25 C. Kunze, T. Freier, E. Helwig, B. Sandner, D. Reif, A. Wutzler and H. J. Radusch, *Biomaterials*, 2003, **24**, 967–974.
26 M. Y. Lu and F. C. Chang, *J. Appl. Polym. Sci.*, 1999, **73**, 2029–2040.
27 G. X. Chen, H. S. Kim, J. H. Shim and J. S. Yoon, *Macromolecules*, 2005, **38**, 3738–3744.
28 F. Y. C. Boey and T. H. Lee, *Polym. Test.*, 1994, **13**, 47–53.
29 M. Vallet-regi, *J. Chem. Soc., Dalton Trans.*, 2001, **100**, 97.
30 W. F. Harrington and P. H. Vonhippel, *Adv. Protein Chem.*, 1961, **16**, 1–138.
31 A. Oyane, M. Uchida, C. Choong, J. Triffitt, J. Jones and A. Ito, *Biomaterials*, 2005, **26**, 2407–2413.
32 S. Liao, M. Ngiam, F. Watari, S. Ramakrishna and C. K. Chan, *Bioinspir. Biomimetics*, 2007, **2**, 37–41.
33 S. Mobini, J. Javadpour, M. Hosseinalipour, M. Ghazi-Khansari, A. Khavandi and H. R. Rezaie, *Adv. Appl. Ceram.*, 2008, **107**, 4–8.
34 A. H. Touny, C. Laurencin, L. Nair, H. Allcock and P. W. Brown, *J. Mater. Sci.: Mater. Med.*, 2008, **19**, 3193–3201.
35 C. X. Resende, J. Dille, G. M. Platt, I. N. Bastos and G. A. Soares, *Mater. Chem. Phys.*, 2008, **109**, 429–435.
36 I. S. Park, U. J. Choi, H. K. Yi, B. K. Park, M. H. Lee and T. S. Bae, *Surf. Interface Anal.*, 2008, **40**, 37–42.
37 C. Combes and C. Rey, *Biomaterials*, 2002, **23**, 2817–2823.
38 M. F. Pittenger, A. M. Mackay, S. C. Beck, R. K. Jaiswal, R. Douglas, J. D. Mosca, M. A. Moorman, D. W. Simonetti, S. Craig and D. R. Marshak, *Science*, 1999, **284**, 143–147.
39 R. F. Service, *Science*, 2000, **289**, 1498–1500.
40 G. J. Rho, B. M. Kumar and S. Balasubramanian, *Front. Biosci.*, 2009, **14**, 3942–3961.
41 H. W. Kim, H. E. Kim and V. Salih, *Biomaterials*, 2005, **26**, 5221–5230.
42 S. Shinzato, T. Nakamura, T. Kokubo and Y. Kitamura, *J. Biomed. Mater. Res.*, 2001, **55**, 277–284.
43 L. M. Siperko, R. Jacquet and W. J. Landis, *J. Biomed. Mater. Res., Part A*, 2006, **78A**, 808–822.
44 J. M. Curran, R. Chen and J. A. Hunt, *Biomaterials*, 2005, **26**, 7057–7067.
45 T. Komori, *Adv. Exp. Med. Biol.*, 2010, **658**, 43–49.
46 G. S. Stein, J. B. Lian, A. J. van Wijnen, J. L. Stein, M. Montecino, A. Javed, S. K. Zaidi, D. W. Young, J. Y. Choi and S. M. Pockwinse, *Oncogene*, 2004, **23**, 4315–4329.
47 H. L. Merriman, A. J. Vanwijnen, S. Hiebert, J. P. Bidwell, E. Fey, J. Lian, J. Stein and G. S. Stein, *Biochemistry*, 1995, **34**, 13125–13132.
48 C. Banerjee, L. R. McCabe, J. Y. Choi, S. W. Hiebert, J. L. Stein, G. S. Stein and J. B. Lian, *J. Cell. Biochem.*, 1997, **66**, 1–8.
49 H. Sun, F. Ye, J. Wang, Y. Shi, Z. Tu, J. Bao, M. Qin, H. Bu and Y. Li, *Transplant. Proc.*, 2008, **40**, 2645–2648.
50 P. Muller, U. Bulnheim, A. Diener, F. Luthen, M. Teller, E. D. Klinkenberg, H. G. Neumann, B. Nebe, A. Liebold, G. Steinhoff and J. Rychly, *J. Cell. Mol. Med.*, 2008, **12**, 281–291.
51 E. Donzelli, A. Salvade, P. Mimo, M. Vigano, M. Morrone, R. Papagna, F. Carini, A. Zaopo, M. Miloso, M. Baldoni and G. Tredici, *Arch. Oral Biol.*, 2007, **52**, 64–73.
52 N. G. Rim, J. H. Lee, S. I. Jeong, B. K. Lee, C. H. Kim and H. Shin, *Macromol. Biosci.*, 2009, **9**, 795–804.
53 S. Rammelt, E. Schulze, M. Witt, E. Petsch, A. Biewener, W. Pompe and H. Zwipp, *Cells Tissues Organs*, 2004, **178**, 146–157.
54 C. G. Pitt, F. I. Chasalow, Y. M. Hibionada, D. M. Klimas and A. Schindler, *J. Appl. Polym. Sci.*, 1981, **26**, 3779–3787.

